

# Early Mesozoic mantle-crust transitional zone in eastern Inner Mongolia: Evidence from measurements of compressional velocities of xenoliths at high pressure and high temperature

SHAO Ji'an (邵济安)<sup>1</sup> & HAN Qingjun (韩庆军)<sup>2</sup>

1. Department of Geology, Peking University, Beijing 100871, China;

2. Institute of Geology and Geophysics, Chinese Academy of Sciences, Beijing 100029, China

Received August 31, 2000

**Abstract** Compression wave velocity  $V_p$  has been measured on 10 representative rock samples from the Early Mesozoic granulite and mafic-ultramafic cumulate xenoliths population from the Harqin area of the Inner Mongolia Autonomous Region (for short Inner Mongolia) as an aid to interpreting *in-situ* seismic velocity data and investigating velocity variation with depth in a mafic lower crust. The experiments have been carried out at constant confining pressures up to 1 000 MPa and temperatures ranging from 20 to around 1 300°C, using the ultrasonic transmission technique. After corrections for estimated *in situ* crustal pressures and temperatures, elastic wave velocities range from 6.5 to 7.4 km · s<sup>-1</sup>, indicating that they are components of the Early Mesozoic crust-mantle transitional zone. Combining with previous experimental data, we have also reestablished the Early-Mesozoic continental compression velocity profile and compared it with those of the present and of the different tectonic environments in the world. The result shows that it is similar to the velocity pattern of the extensional tectonic area, providing new clues to the Mesozoic continental structure of the North China Craton.

**Keywords:** eastern Inner Mongolia, Early Mesozoic, crust-mantle transitional zone, high temperature and high pressure, compressional wave velocity.

The “Mantle-crust transition” has received increasing attention of geologists in recent years. It is defined as a zone with P-wave velocities ranging from 6.8—7.8 km/s, just between those of crust ( $V_p = 5.8—6.5$  km/s) and mantle (8.0—8.3 km/s) classified according to classic geophysics<sup>[1]</sup>. More than 90 refraction profilings in continental area and elastic velocities measurements in lab of a large variety of lithologic samples demonstrate up to 94% of velocities in the former-believed lower crust change between 6.4 and 7.4 km/s<sup>[2]</sup>, suggesting that the mantle-crust transitional zones spread globally. Moreover, lots of researches show a close relationship between the structure of the mantle-crust transition and regional tectonic settings and geological evolutionary history<sup>[3]</sup>.

Xenoliths brought to the earth's surface by magmas of deep-seated origin, outcropped and high-grade metamorphic terranes, and mantle crust transition zone sheets thrust to the surface by tectonic movement can be used as important “lithoprobe” to measure directly their elastic properties under high pressure and high temperature and determine their compositions *in situ*

conditions successfully<sup>[4–7]</sup>. It is clear that these ways combining with other geophysical methods (e.g. reflection and refraction profiling) can provide more detailed clues to the structure and composition of the continental lithosphere.

A large amount of xenoliths have been discovered in a series of the Early Mesozoic diorites (221–205 Ma) in the Harqin area in eastern Inner Mongolia, North China. The population of xenoliths can be divided into three types according to different petrogeneses: (1) cumulates<sup>[8]</sup>; (2) mafic granulites<sup>[9]</sup>; (3) amphibolite facies metamorphic rocks. As non-roofed fragments in the host diorites, most xenoliths are fresh showing little alteration and varying largely in shape and size. Preliminary study suggests that the cumulates were products of mantle-derived magma underplating in the Early Mesozoic (241–214 Ma)<sup>[8]</sup>. Granulite xenoliths experienced high-grade metamorphism roughly at the same time (Early Mesozoic). Both mineral chemistry and equilibrated P-T conditions (800–950°C, 0.7–1.1 GPa) of the granulite xenoliths differ from those of Archean terrain granulites exposed on the surface of the North China Craton, suggesting the different petrogeneses and metamorphic evolutionary history<sup>[9]</sup>. They thus together form a relatively intact deep crust profile in the Early Mesozoic and provide an excellent opportunity to investigate its mantle-crust structure. We report here the measurements of ultrasonic P-wave velocities under high pressure and high temperature of the representative lower crustal xenoliths. On the basis of the  $V_p$  results, we intend to reconstruct the Early Mesozoic mantle-crust structure and discuss its implications for lithospheric evolution of the North China Craton.

## 1 Samples and experimental technique

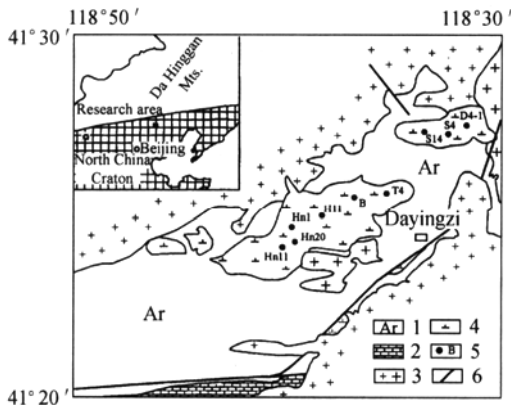


Fig. 1. Geological sketch of the research area and sampling locality. 1, Archaeozoic metamorphic rocks; 2, Proterozoic Changcheng System; 3, Mesozoic granites (left) and Paleozoic granites (right); 4, Early Mesozoic diorites; 5, sampling localities and numbers; 6, faults.

The suite of the lower crustal xenoliths investigated here include two pyroxenes, a gabbro, a troctolite, an anorthosite, three mafic granites and a peridotite nodule. Fig. 1 shows sampling locality. They are all free from visible fractures and, when possible, secondary alterations with an exception of serpentinization in the spinel peridotite. The rock types and the modal analyses of the samples are given in table 1. Their whole rock major element chemical composition, and bulk densities under room temperature are listed in table 2.

The P-wave velocity experiments were performed in a high-temperature and high-pressure cell in the so-called YJ-3000 ton (pressure source with precision within 0.01 GPa) equipped with a wedge-type cubic anvil at Guiyang Institute of Geochemistry, the Chinese Academy of

Table 1 Rock types and modal analyses (vol.%)

Sample No.	Rock type	Modal composition (%)
S4	spinel peridotite	Ol (47) + Opx (15) + Cpx (12) + Ser (24) + (Phl+ Spl + Mt)
T4	pyroxenite	Ol (15) + Opx (48) + Cpx (36) + (Phl + Spl + Mt)
S14	olivine pyroxenite	Opx (40) + Cpx (32) + Olv (25) + (Plg + Phl + Mt + Spl)
H11	gabbro	Plg (62) + Opx (7) + Cpx (30) + Amp (<1)
B	troctolite	Plg (60) +Olv (22) + Cpx (13) + (Phl +AmP)
D4-1	anorthorite	Plg (>98) + (Mt +Zr)
Hn11	two-pyroxene granulite	Plg (58) + Cpx (20) + Opx (20) + (Bi + Mt + Zr)
Hn1	two-pyroxene granulite	Plg (58) + Cpx (18) +Opx (22) + Bi (<2) + (Mt + Zr)
Hn20	hypersthene granulite	Plg (54) + Opx (30) + Bi (8) + (Mt + Zr) + Qz (6)

Ol, olivine; Opx, orthopyroxene; Cpx, clinopyroxene; Plg, plagioclase; Bi, biotite; Phl, phlogopite; Qz, quartz; Spl, spinel; Mt, magnetite; Zr, zircon; Ser, serpentine.

Table 2 Chemical analyses of major oxides (wt.%) and densities of the samples

No.	T4	S4	B	H11	D4-1	S14	Hn1	Hn11	Hn20
SiO <sub>2</sub>	48.91	43.10	49.78	51.11	56.87	50.19	48.55	52.34	50.85
TiO <sub>2</sub>	0.37	0.23	0.10	0.48	0.06	0.59	0.39	0.38	1.46
Al <sub>2</sub> O <sub>3</sub>	4.15	2.84	24.29	20.85	26.05	5.70	14.42	13.72	16.98
Fe <sub>2</sub> O <sub>3</sub>	4.61	2.57	0.53	1.28	0.41	5.33	0.96	0.41	2.76
FeO	5.28	9.11	2.35	2.03	0.18	4.33	7.38	7.53	8.02
MnO	0.16	0.22	0.04	0.06	0.01	0.15	0.26	0.27	0.24
MgO	20.64	33.33	6.05	5.35	0.24	19.58	12.57	11.19	8.36
CaO	12.66	2.63	11.62	13.14	8.33	9.42	10.84	8.54	5.33
Na <sub>2</sub> O	0.69	0.19	2.95	2.55	5.07	0.81	1.32	0.62	0.68
K <sub>2</sub> O	0.63	0.14	0.33	0.46	1.16	0.70	1.33	2.55	2.96
P <sub>2</sub> O <sub>5</sub>	0.08	0.05	0.04	0.05	0.03	0.09	0.10	0.10	0.71
Loss	1.19	5.78	1.53	2.29	0.99	2.63	1.61	1.83	1.15
Total	99.37	100.19	99.61	99.65	99.39	99.52	99.73	99.48	99.50
$\rho$	3.163	3.042	2.890	2.808	2.648	3.225	3.016	2.937	2.934

Chemical compositions were analyzed by Cao Jie using standard XRF method at Institute of Geology and Geophysics of the Chinese Academy of Sciences. Densities at room temperature were calculated by measuring volume and mass.

Sciences. Xie et al.<sup>[10]</sup> and Xu et al.<sup>[11]</sup> documented the detailed experimental installation. The cylindrical sample (12 mm in diameter and 32 mm in length) with double stainless-steel foils heater is placed in the center of pyrophyllite cube (32 mm×32 mm×32 mm) as a pressure transmitting medium. Two P-wave Transducers are stacked on center position of the backs of the upper and the lower anvils separated by epoxy resin, and the centers of the transducers and sample are in alignment. The two transducers are linked with emitting and receiving parts of a sound wave detective meter (SD-1). The transducers are made of PZT ceramics, 10 mm in diameter and 1 MHz in frequency. The change of the length of samples is monitored constantly through measuring the upper and lower anvils by an electrical inductive dilatometry whose sensitivity is 0.01mm. Before experiment, the calibrations of temperature and pressure in cell have been done. The temperature of cell is obtained from a Pt<sub>90</sub>Rh<sub>10</sub>-Pt thermocouple with uncertainty less than 5°C. The pressure of cell is calibrated by observing the phase changes of quartz-coesite and according to copper melting curve<sup>[11]</sup>. The accuracy of pressure measurement is believed to be better than 1%. At first,  $V_p$  on samples is measured by club-transducers at room temperature and 10<sup>5</sup> Pa, then the sample is amounted in cell. After SD-1 ultrasonic detector is powered, press is started to make the pressure of cell go up to expected value at a constant rate of 0.1 GPa per 10

min. When the pressure of cell has been stable for 10 min, cell is heated up to expected value at a constant rate of 5°C/s. When both the pressure and temperature have been stable for 35 min, the travel time of P-wave can be measured in SD-1. In the procedure of the experiment, oxygen fugacity is not controlled. Because no obvious preferred mineral orientation or compositional layering in the samples, all experiments are conducted in one direction and the velocity anisotropy is not taken into consideration.

## 2 Results

### 2.1 Velocity-pressure relationship at room temperature

Velocities measured on rock samples at atmospheric pressure are very strongly sensitive to the presence of open cracks and grain boundaries. In order to measure velocities that reflect the intrinsic properties of the assemblage of minerals, it is therefore essential for the samples to bear at least a few hundred MPa of confining pressure in order to close the voids in the samples. Many studies<sup>[4,6,7]</sup> have demonstrated that the majority of the cracks and grain boundaries in most igneous and metamorphic rocks are closed at confining pressures more than 200–400 MPa, although further closure, presumably of microcracks, continues to pressures of at least 1 000 MPa. For the purpose of the present study, the velocity measurements were conducted up to 1 000 MPa with one exception (up to 1 100 MPa).

The pressure dependence of P-wave velocity at room temperature for the different rock types is shown in fig. 2 (tabulated original data are available on request). In the low-pressure range, P-wave velocities of most samples increase rapidly with increasing confining pressure, reflecting the closure of flat microcracks. However, within 0–200 MPa,  $V_p$  of samples B, Hn20 and Hn1

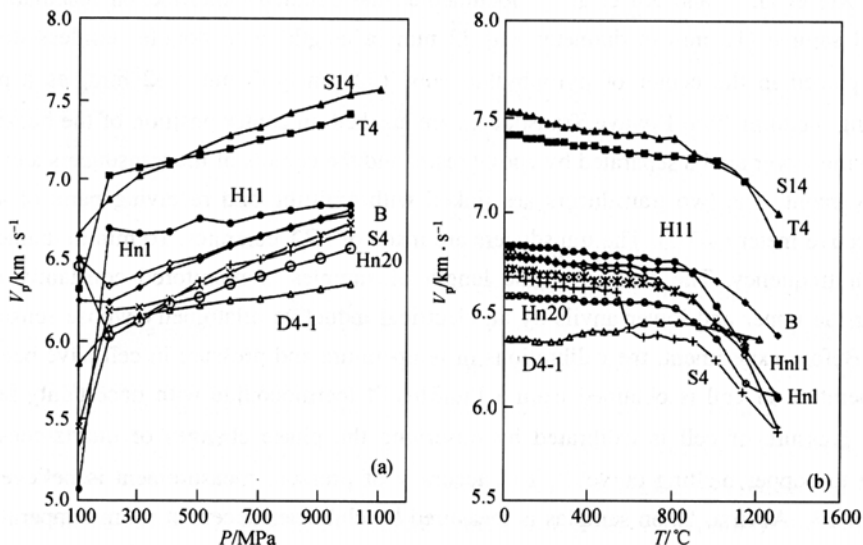


Fig. 2. Variations in wave velocity of the samples with pressure at room temperature (a) and with temperature at 1 GPa (b).

decreases as the confining pressure increases, especially Hn20 from 6.46 to 6.03 km/s. It probably suggests that in the early experimental stage these three samples may experience a process from crushing to concretion in which their  $V_p$  decreases and then increases. Above about 200 MPa, the correlations between velocity and confining pressure become nearly linear, indicating that intrinsic velocities are approached.

It is clear from fig. 2(a) that different rock types show large variations in P-wave velocity at higher pressure. At 1000 MPa confining pressure, P-wave velocities range from 6.57 to 6.80 km/s for mafic granulites, 6.77–6.83 km/s for mafic cumulates. Pyroxenite and olivine pyroxenite show the highest  $V_p$  from 7.34–7.53 km/s, while anorthosite and spinel peridotite have lower  $V_p$ , 6.35 km/s and 6.67 km/s respectively. Variation in elastic wave velocities is closely related to the modal compositions of the rocks and to the respective single crystal velocities (see table 1). Abundant olivine and pyroxene explain high P-wave velocities of ultramafic rocks. Abundant modal plagioclase and some hydrous minerals such as hornblende and biotite (phlogopite) are responsible for medium-low range velocities of P-wave of mafic cumulate and granulite xenoliths. The peridotite sample (S<sub>4</sub>) is strongly serpentinized that explains the anomalously low  $V_p$ <sup>[12,13]</sup>.

## 2.2 Velocity-temperature relations at 1 000 MPa confining pressure

Since elastic wave velocities are very sensitive to microfracture, the intrinsic effects of temperature on  $V_p$  can only be obtained at pressures that suppress the opening of microcracks. The minimum pressure increment to prevent thermal cracking has been estimated to be around 1 MPa per degree increase in temperature<sup>[14]</sup>. But, taking *in situ* P-T conditions of the lower crustal xenoliths into consideration, all velocity measurements as a function of temperature were carried out at high constant confining pressure of 1 000 MPa.

Fig. 2(b) shows the plot of P-wave velocities versus temperature at 1 000 MPa. In general, the linear behavior is observed up to 800°C, however, the slopes become more and more nonlinear, indicating the onset of thermal cracking<sup>[4,7]</sup>. Xu et al. called it “sound soften”<sup>[11]</sup>.  $V_p$  in the serpentine-bearing peridotite shows a significant abrupt drop at around 550°C. This phenomenon was also found by Kern et al.<sup>[6]</sup>. It may be attributed to the breakdown of mineral serpentine and a minor amount of phlogopite. The dehydration reaction produces solid-fluid systems and as a consequence effective pressure decreases, thereby leading to the formation of new microcracks and a reconstitution of the pore geometry. Differing from the other samples,  $V_p$  of anorthosite (D4-1) shows a positive linear trend with temperature increasing. This probably reflects that the relatively homogeneous composition of the anorthosite restrains thermal-inducing microcracks and boundary effect that can make  $V_p$  decrease.

## 2.3 Calculation of P-wave velocity of samples at high temperature and high pressure

Correction of the elastic wave velocities to the lower crust requires knowledge of pressure and temperature derivatives of the wave velocities and the inferred *in situ* P-T conditions of the

samples. Previous study has suggested an extensional tectonic environment for the North China Craton in the Early Mesozoic with the end of collisional mountain-building<sup>[15]</sup>. Thus we assume that the geotherm was 60 mW/m<sup>2</sup>, similar to the average geotherm of American Basin and Range Province<sup>[16]</sup>. In addition, this value is also near the present geotherm (60—65 mW/m<sup>2</sup>) of the research area where geophysics data show that present temperature at Moho is around 600°C and the average temperature of the lower crust is about 500°C<sup>[17]</sup>. The estimated equilibrated pressure for the mafic granulite xenoliths ranges from 0.7 to 1.1 GPa<sup>[9]</sup>. Beneath them are cumulates formed by the magmatic underplating. Both the two kinds of xenoliths are components of the lowest continental crust. Therefore, we assume the *in situ* P-T conditions for calculation of the Early Mesozoic P-wave velocities of the samples to be 400°C, 0.7 GPa and 600°C, 1.0 GPa.

The pressure and temperature derivatives of P-wave velocities have been calculated using best-fit solutions from the linear part of the velocity-pressure and velocity-temperature relations (see fig. 2(a), (b)) which are considered to reflect the intrinsic properties of the compact aggregates. The results are listed in table 3. Also listed are the *in situ* P-wave velocities that were calculated using the formula proposed by Kern et al.<sup>[6,7]</sup>.

Four instinct features are shown in table 3: (1) as the temperature and pressure increase, the  $V_p$  correspondingly increases; (2)  $V_p$  of most samples ranges from 6.5—7.4 km/s; (3)  $V_p$  of the cumulates is higher than that of the granulites; (4) strongly serpentinized spinel peridotite has an anomalously low  $V_p$ . Because  $V_p$  of most samples is higher than that of the crust (<6.5 km/s) but lower than that of the mantle (>8 km/s), it is considered that they are all components of the mantle-crust transitional zone. Hydrous minerals including mica and/or amphibole commonly contained in most studied rock samples may reduce P-wave velocity. In addition, the protoliths of the granulite xenoliths are believed to be basaltic rocks and their composition and equilibrated P-T conditions differ from those of Archean terrain granulites exposed on the surface of the North China Craton. Thus we take both the cumulate and mafic granulite xenoliths as the components of the mantle-crust transition.

Table 3 Pressure and temperature derivatives of P-wave velocities and  $V_p$  in inferred *in situ* conditions

No.	Rock type	$V_{p_0}$ /km · s <sup>-1</sup>	$\frac{dV_p}{dP} \times 10^4$	$\frac{dV_p}{dT} \times 10^4$	$V_{p_1}$ /km · s <sup>-1</sup>	$V_{p_2}$ /km · s <sup>-1</sup>
		(0 MPa, 0°C)	/km · s <sup>-1</sup> · MPa <sup>-1</sup>	/km · s <sup>-1</sup> · °C <sup>-1</sup>	(700 MPa, 400°C)	(1000 MPa, 600°C)
Hn20	hypersthene granulite	5.92	6.52	-0.63 (22—821°C)	6.38	6.53
Hn11	two-pyroxene granulite	6.00	7.08	-1.18 (22—737°C)	6.45	6.64
Hn1	two-pyroxene granulite	6.55	5.68	-1.92 (24—737°C)	6.55	6.68
D4-1	anorthorite	6.03	3.00	+1.23 (26—932°C)	6.29	6.40
B	troctolite	6.11	6.68	-0.81 (21—815°C)	6.55	6.77
H11	gabbro	6.62	2.25	-1.11 (23—815°C)	6.73	6.83
T4	pyroxenite	7.21	4.72	-1.49 (24—1015°C)	7.21	7.32
S14	olivine pyroxenite	6.78	7.53	-1.93 (24—815°C)	7.23	7.42
S4	spinel peridotite	5.88	7.92	-1.55 (21—541°C)	6.37	6.58

## 2.4 Reconstruction of the Early Mesozoic mantle-crust transition and its geological implications

The construction of the Early Mesozoic mantle-crust transition has a key important role in deducing the tectonic evolutionary history in the research area and even in the North China Craton. The researched Harqin area is located in the east of North-China Craton and right in the uplift (so-called “Inner Mongolia Earth Axis”) at north edge of the North China Craton. In the Pre-Mesozoic it is mainly composed of Archean metamorphic rocks<sup>[18]</sup>. A small part of the Proterozoic Changcheng System is distributed in the south of the study area. According to the data from the comparable Jidong (eastern Hebei Province) area, the Pre-Cambrian has a thickness of around 25 948 m<sup>[19]</sup>. At Qingshan Town in the Harqin area, 910—1 410 m thick Cambrian is also distributed from the 1/200 000 regional geological survey data. We can estimate the thickness of the Pre-Mesozoic as 27 km in the study area. Taking input of magma into consideration, we assume the thickness of Pre-Mesozoic to be 30 km. The equilibrated pressure (<1 GPa) of the Early Mesozoic granulite xenoliths<sup>[9]</sup> indicates the lowest thickness of 32 km. Clinopyroxene geobarometer of magmatic rocks proposed by Nimis<sup>[20]</sup> gives an estimate of the cumulates formed thickness ranging from 33 to 36 km. Thus we can get a rough thickness of 36 km for the crust including the mantle-crust transition in the Early Mesozoic for the research area.

There are mounting evidences from crust seismic studies that give a three-layered crustal model with a thickness of the crust ranging from 36 to 38 km in the area<sup>[21,22]</sup>. Noticeable are two features: (1) a relatively low  $V_p$  (6.0 km/s, roughly similar to that of granites) layer in the middle crust level, with its geological meanings unclear; (2) a high  $V_p$  (6.8—7.55 km/s) layer with a thickness of 2 km in the base of the lower crust, believed to represent the present mantle-crust transitional zone.

Combining  $V_p$  of these samples from the lower crust with previous laboratory measurements, we reconstruct the  $V_p$ -depth profile of Early Mesozoic crust (fig. 3). For comparison, the crust P-wave velocity patterns for the present studied area<sup>[23,24]</sup> and typical tectonic provinces including orogens, rifts, shields and platforms<sup>[13]</sup> are also given in fig. 3. It is clear from the figure that both the thickness and  $V_p$ -depth profile of the Early Mesozoic crust in the study area are similar to those of the present crust. It may suggest that the influences of crustal accretion<sup>[25]</sup> and crust thinning marked by large-scale detachment-metamorphic core complex<sup>[26]</sup> since the Mesozoic on the crustal thickness and  $V_p$ -depth structure of the North China Craton counteract each other. In comparison with typical tectonic provinces in the world, both the crustal thickness and  $V_p$ -depth profile of Harqin area are similar to those of continental rifts with the exception of a thinner high  $V_p$  layer in the lower crust, while differ distinctly from those of orogens, shields and platforms. Most recently, Zhao et al.<sup>[3]</sup> studied the present mantle-crust transition in Liaodong-Yanshan area, and pointed out that the Moho here appears as a first-class discontinuity reflecting an extensional tectonic environment. They even considered that Yanshan fold belt used to be a Mesozoic rift.

The above discussion on the crustal thickness and  $V_p$ -depth profile suggests an extensional

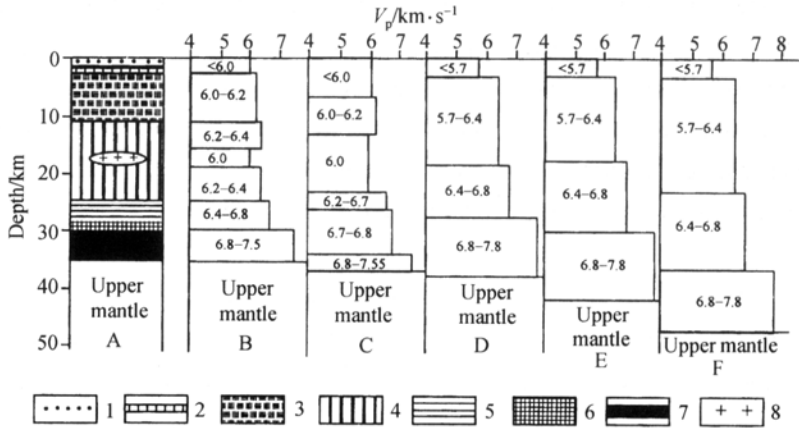


Fig. 3. Lithology-wave velocity-depth profiles of the research area in Early Mesozoic (taken from ref. [23]) and its comparison with the typical crustal wave velocity patterns of the present world (taken from ref. [13]). A, Lithology-depth profile of the research area in Early Mesozoic; B, crustal wave velocity-depth profile of the research area in Early Mesozoic; C, crustal wave velocity-depth profile in the present; D, typical crustal wave velocity pattern in rift areas; E, typical crustal wave velocity pattern in shield and craton areas; F, Typical crustal wave velocity pattern in orogenic belts; 1, Palaeozoic; 2, Proterozoic Changcheng System; 3, Archaeozoic supracrustal rocks; 4, Archaeozoic orthometamorphite, mainly TTG rocks; 5, Archaeozoic granulites; 6, Early Mesozoic granulites; 7, mafic-ultramafic cumulates; 8, Paleozoic granites.

tectonic environment in the study area in the Early Mesozoic. This opinion is also supported by other geological and geochemical researches<sup>[27, 28]</sup>. Recent researches on the Late Triassic to Early-Middle Jurassic mafic-ultramafic rocks and mafic dyke swarms from the North China Craton and the mid-south section of the Da Hinggan Mts. also suggested that North China Craton had been in an extensional setting since the Early Mesozoic<sup>[15, 29–31]</sup>.

Laboratory measurements of P-wave velocity at high-temperature and high-pressure on 10 representative rock samples from the Early Mesozoic granulite and mafic-ultramafic cumulate xenoliths from Harqin area of the eastern Inner Mongolia affirm the existence of the mantle-crust transitional zone. And on this basis, we reconstruct tentatively the  $V_p$ -depth profile of the Early Mesozoic crust. Certainly, many problems involving lithospheric composition, geothermal state and their geotectonic setting need further research and even more multidisciplinary cooperation. In the past, most geologists did not attach importance to the tectonic evolution of north China in the Early Mesozoic. As a matter of fact, the composition, structure and evolution of the North China Craton in the Early Mesozoic can provide most important clues to the intensive magmatic activity of the North China Craton in the Mesozoic, and thus should attract more attention.

**Acknowledgements** This work was supported by the National Natural Science Foundation of China (Grant No. 49672156).

## References

- Deng, W., Zhong, D., Mantle-crust transitional zone and its geological implications in lithosphere tectonic evolution, Chinese Science Bulletin (in Chinese), 1997, 42(23): 2474.
- Holbrook, W. S., Mooney, W. D., Christensen, N. I., The seismic velocity pattern of the deep continental crust, Continental



- Lower Crust (eds. Fountain, D. M. et al.), Amsterdam: Elsevier, 1992, 1—43.
3. Zhao, J., Zhang, X., Zhao, G. et al., Structure of crust-mantle transitional zone in different tectonic environments, *Earth Science Frontiers* (in Chinese with English abstract), 1999, 6(3): 165.
  4. Christensen, N. I., Fountain, D. M., Constitution of the lower continental crust based on experimental studies of velocities in granulite, *Geol. Soc. Am. Bull.*, 1975, 86: 227.
  5. Fountain, D. M., The Ivrea-Verbano and Strona-Ceneri zones northern Italy: a cross-section of the continental crust—new evidence from seismic velocities of rock samples, *Tectonophysics*, 1976, 33: 145.
  6. Kern, H., Schenk, V., Elastic velocities in rocks from a lower crustal section in southern Calabria (Italy), *Phys. Earth Planet. Inter.*, 1985, 40 :147.
  7. Kern, H., Schenk, V., A model of velocity pattern beneath Calabria, southern Italy, based on laboratory data, *Earth Planet. Sci. Lett.*, 1988, 87: 325.
  8. Shao, J., Han, Q., Zhang, L. et al., Cumulate complex xenoliths in the Early Mesozoic in eastern Inner Mongolia, *Chinese Science Bulletin*, 1999, 44(14): 1272.
  9. Han, Q., Shao, J., Mineral chemistry and metamorphic *p-t* conditions of granulite xenoliths in Early Mesozoic diorite in Harqin region, Eastern Inner Mongolia Autonomous Region, China, *Earth Science—Journal of China University of Geosciences* (in Chinese with English abstract), 2000, 25(1): 21.
  10. Xie, H., Zhang, Y., Xu, H. et al., A new method of measurement for elastic wave velocities in minerals and rocks at high temperature and high pressure and its significance, *Science in China, Series B*, 1993, 36(10): 1276.
  11. Xu, J., Zhang, Y., Xu, H., Guo, J. et al., Measurements of ultrasonic wave velocities at high temperature and high pressure for window glass, pyrophyllite, and kimberlite up to 1 400°C and 5.5 GPa, *High Temperature-High Pressure*, 1994, 26: 375.
  12. Robert, S. C. (ed.), *Practical Handbook of Physical Properties of Rocks and Minerals*, Boca Raton Florida: CRC Press, 1989, 517—531.
  13. Christensen, N. I., Mooney, W. D., Seismic velocity pattern and composition of the continental crust: a global review, *J. Geophys. Res.*, 1995, 100(B6): 9761.
  14. Kern, H., Ritche, A., Temperature derivatives of compressional and shear wave velocities in crustal and mantle rocks at 6 kbar confining pressure, *J. Geophys.*, 1981, 49: 47.
  15. Shao Ji'an, Mu Baolei, He Guoqi et al., Geological effects in tectonic superposition of Paleo-Pacific domain and Paleo-Asian domain, *Science in China, Series D*, 1997, 40(6): 634.
  16. Furlong, K. P., Fountain, D. M., Continental crustal underplating: thermal considerations and seismic-petrological consequences, *J. Geophys. Res.*, 1986, 91(B8): 8285.
  17. Wang, J. (ed.), *Geothermics in China*, Beijing: Seismological Press, 1996.
  18. Wang, S., Sun, C., Cui, W. et al., *Gold Mine Geology in Chifeng Area, Eastern Inner Mongolia* (in Chinese), Hohhot: People's Publishing House of Inner Mongolia, 1994.
  19. Cheng, Y. (ed.), *Chinese Regional Geology* (in Chinese), Beijing: Geological Publishing House, 1994, 429.
  20. Nimis, P., Clinopyroxene geobarometry of magmatic rocks, Part 2., Structural geobarometers for basic to acid, tholeiitic and mildly alkaline magmatic systems, *Contrib. Mineral. Petrol.*, 1999, 135: 62.
  21. Yuan Xuecheng, *Altas of Geophysics in China*, Beijing: Geological Publishing House, 1996.
  22. *Geoscience Transect Editorial of Chinese Seismic Bureau*, *Geoscience transects from Suizhou of Hubei Province to Harqin of Inner Mongolia* (in Chinese), Beijing: China Seismological Press, 1992.
  23. Gao, L., Ge, H., Preliminary study of elastic wave velocity of rock samples at high pressure from China continent, *Acta Geophysica Sinica* (in Chinese with English abstract), 1975, 18: 26.
  24. Hao, J., Liu, X., Li, J., Experimental measurements of density and elastic wave velocity at 10 kbar of typical rocks from north China, *Acta Seismologica Sinica* (in Chinese with English abstract), 1985, 7(3): 276.
  25. Shao, J., Han, Q., Zhang, L. et al., Two kinds of vertical accretion of the continental crust: an example of the Da Hinggan Mts, *Acta Petrologica Sinica* (in Chinese with English abstract), 1999, 15(4): 600.
  26. Fu, C., Metamorphic core complex of Hebei Province, *Collection of Geological Prospecting* (in Chinese), 1999, 14(3): 10.
  27. Ma, W., Liu, A., The Xishan of Beijing—a part of an aulacogenient in Early Mesozoic, *Scientia Geologica Sinica* (in Chinese with English abstract), 1986, 1: 54.
  28. Mu, B., Yan, G., Geochemistry of Triassic alkaline or subalkaline igneous complexes in the Yan-Liao area and their significance, *Acta Geologica Sinica* (in Chinese with English abstract), 1992, 66(2): 108.
  29. Shao, J., Zhang, L., Mu, B., Tectono-thermal evolution of middle-south section of the Da Hinggan Mountains, *Science in China, Ser. D*, 1998, 41(6): 570.
  30. Shao, J., Zhang, L., Mu, B., Magmatism in the Mesozoic extending orogenic process of the Da Hinggan Mts, *Earth Science Frontiers* (in Chinese with English abstract ), 1999, 6(4): 339.
  31. Shao, J., Mu, B., Zhang, L., Deep geological process and its shallow response during Mesozoic transfer of tectonic frameworks in eastern North China, *Geological Review* (in Chinese with English abstract), 2000, 46(1): 32.